



HAL
open science

ICRF heating and turbulent transport modelling of the WEST L-mode plasma using ETS: interpretative and predictive code validation

P Huynh, E Lerche, D van Eester, J Garcia, G Frazzoli, P Maget, J F Artaud, J Ferreira, T Johnson, D Yadykin, et al.

► To cite this version:

P Huynh, E Lerche, D van Eester, J Garcia, G Frazzoli, et al.. ICRF heating and turbulent transport modelling of the WEST L-mode plasma using ETS: interpretative and predictive code validation. 48th EPS conference on plasma physics, Jun 2022, Maastricht (Virtual event), Netherlands. cea-03740616

HAL Id: cea-03740616

<https://cea.hal.science/cea-03740616>

Submitted on 29 Jul 2022

HAL is a multi-disciplinary open access archive for the deposit and dissemination of scientific research documents, whether they are published or not. The documents may come from teaching and research institutions in France or abroad, or from public or private research centers.

L'archive ouverte pluridisciplinaire **HAL**, est destinée au dépôt et à la diffusion de documents scientifiques de niveau recherche, publiés ou non, émanant des établissements d'enseignement et de recherche français ou étrangers, des laboratoires publics ou privés.

ICRF HEATING AND TURBULENT TRANSPORT MODELLING OF THE WEST L-MODE PLASMA USING ETS: INTERPRETATIVE AND PREDICTIVE CODE VALIDATION

P. Huynh¹, E.Lerche^{2,3}, D. Van Eester³, J. Garcia¹, G. Frazzoli¹, P.Maget¹, J.F. Artaud¹, J. Ferreira⁴, T. Johnson⁵, D. Yadykin⁶, P. Strand⁶ and WEST team*

¹ CEA, IRFM, F-13108 Saint Paul-lez-Durance, France

² CCFE, Culham Science Centre, Abingdon OX14 3DB, United Kingdom

³ Laboratory for Plasma Physics, ERM/KMS, B-1000 Brussels, Belgium

⁴ IPFN, Instituto Superior Tecnico, Universidade de Lisboa, 1049-001 Lisbon, Portugal

⁵ KTH, Royal Institute of Technology, Stockholm, Sweden,

⁶ Chalmers University of Technology, Gothenburg, Sweden

* see <http://west.cea.fr/WESTteam>

Abstract. The European Transport Simulator (“ETS”) [1] is a suite of codes designed to simulate tokamak plasma discharges. Not only it highlights the evolution of particle density and energy due to transport effects accounting for particle, heat and current sources, but it equally provides insight into fast ion dynamics resulting from ICRH (and - if present – beams), and the impact these high-energy populations have on the plasma core [2]. This tool allows to help understand the plasma dynamics in WEST and is being used for optimizing the plasma discharge. In particular, attention is being devoted to identify means to avoid a radiative collapse by ensuring an efficient electron RF induced heating and to help finding favourable conditions to enable the L-H transition. The first step was to verify and validate the simulator in interpretative and predictive mode for some relevant WEST L-mode plasmas. Cyrano [5] and StixRedist [6] are used as ICRH modules [2, 7, 8], while transport is assumed to be due to turbulence and is described exploiting the TGLF module [9, 10]. Collisional electron power computed with the ICRF modules was compared with the experimental one obtained by using the Break In Slope method. Scans in minority density and ICRF power were performed in interpretative mode in order to determine the electron/ion heating ratio, revealing dominant electron heating and highlighting that the neutron rate is a sensitive function of the power absorbed by the deuterons. Seeking for the highest possible compatibility between the various available measurements (electron temperature profiles, stored energy and neutron rate) while staying within realistic error bars, predictive modelling which describes the evolution of particle density and temperatures allows to estimate the ion temperature profiles (not yet available on WEST) and to establish a firm link between the WEST experimental data (e.g. energy & neutron rate) on the one hand and the thermal and fast particle profiles resulting from simulation on the other.

INTRODUCTION & BACKGROUND

WEST [3, 4] is a superconducting device, equipped with actively cooled divertor in full tungsten environment. In this paper, D-D L-mode discharges in the flat top phase with ICRH additional heating are considered. The European Transport Simulator (ETS) [1, 2] can simulate full plasma discharges of any Tokamak device. Two main modules are concerned: Cyrano [5] and StixRedist [6, 7, 8] as ICRF module and TGLF [9, 10] as turbulent transport module. The final goals are to understand the core plasma dynamics in WEST with focus on the role of ICRH and the plasma discharge optimization (efficient electron heating, avoid tungsten accumulation). First steps were to verify and validate ICRF modules, determine the electron/ion heating ratio with minority and power scans, compare predictive simulation with experiments and characterize the turbulence.

ICRH MODULES USED IN INTERPRETATIVE MODE

Cyrano/StixRedist was compared to EVE/AQL [11, 12] on the shot #55799 giving a good agreement on the heating profiles (not shown). Then it was compared with the Break In Slope (BIS) experimental profiles from ECE data for the shot #54633 with 1MW of ICRF power. To interpret the experimental power deposition profile in WEST, one needs to invoke the

impact of transport. *Figure 1* shows that reasonable agreement can be obtained when a characteristic time of the order of few tens of ms is considered.

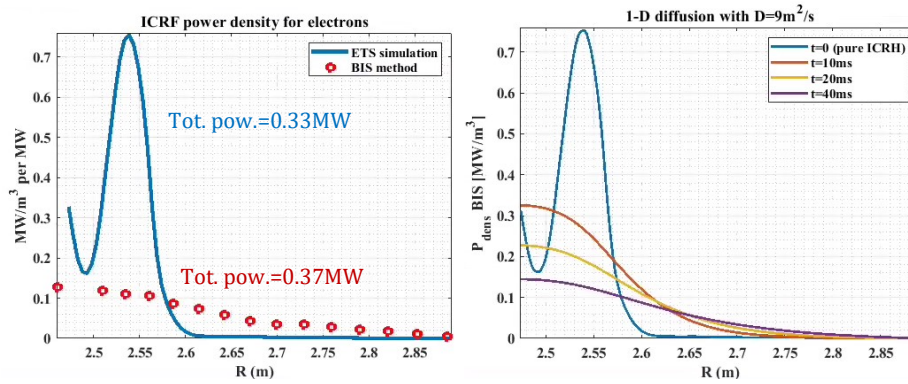


Figure 1: shot #54633 at 39s. (Left) comparison of ICRF electron power density profile between BIS method and ETS interpretative simulation and their integration over the plasma volume. (Right) Imitating BIS method with 1-D diffusion equation. Diffusion coefficient estimated at $9\text{m}^2/\text{s}$ from radial propagation of a sawtooth crash. ICRF electron heat diffusion for various time slice.

An ion temperature measurement is not yet available at WEST. An estimate is made based on the measured neutron rate (assuming Maxwellian ion distribution functions) [13]. Table 1 shows the high sensitivity of the neutron rate for typical T_i values in WEST due to the steep D-D fusion cross section as shown in *fig. 2*.

	Experiment	100% T_i	90% T_i	80% T_i	~60% T_i
Neutron rate (10^{11} neutrons/s)	~27	~57	~32	~17	~2
Discrepancy		111%	18%	-37%	-92%

Table 1: shot #55607 at 39s. Neutron rate sensitivity according to ion temperature amplitude.

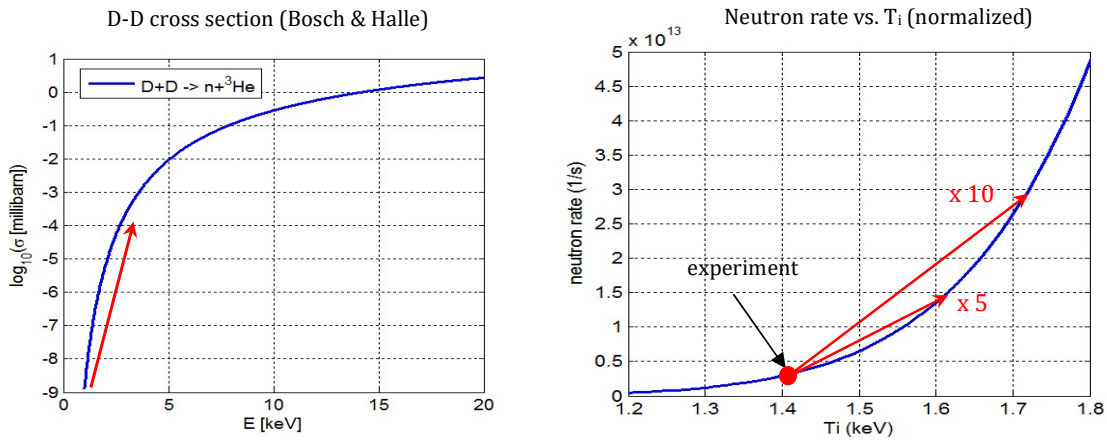


Figure 2: shot #55607 at 39s. (Left) Stiff D-D cross section at the interest region. (Right) Variation of neutron rate according to ion temperature

A minimization loop with Cyrano/StixRedist accounting for ICRF heated deuterium distributions and neutron rate computations suggests T_i to be 12% (1.26 keV) lower than the value obtained assuming purely Maxwellian distributions.

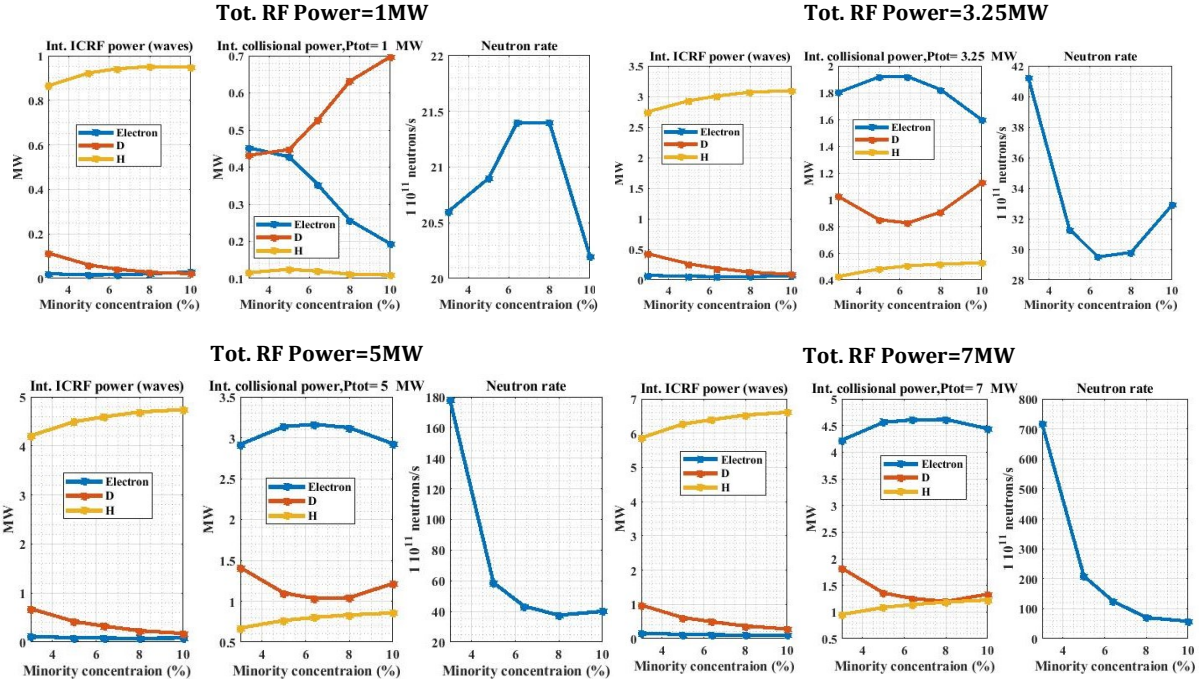


Fig 3: shot #55607 at 39s. H Minority scan for various ICRF power. For each power, plots of integrated direct absorption power, integrated collisional power and neutron rate.

Figure 3 shows that for low power (1MW), the collisional ion heating is dominant but the power is too low to impact the D-D neutron rate. For higher power (>3MW), electron heating is dominant but ion heating is strong enough to enhance the neutron rate, in particular at low concentration (enhanced N=2 D absorption). The neutron rate is limited at large H fraction due to dilution. The neutron enhancement comes from ICRF induced deuterium tails (thermal T_i constant). Note that finite orbit width effects and ripple losses, not taken into account here, can significantly impact the ICRF power absorption profiles at high power and low H concentration [13].

TRANSPORT MODELLING

The kinetic profiles are predicted with NCLASS and TGLF respectively for computing the neoclassical and turbulent transport coefficients. The values of T_e , T_i , N_e and N_i are imposed at normalized $\rho=0.8$ as boundary condition where ρ is the normalized square root of toroidal flux. Impurity radiation profiles are prescribed from the bolometry data. Due to the presence of sawteeth up to $\rho=0.35$, ad-hoc transport coefficients are manually set to fit the electron temperature and density experimental data in that region. The initial T_i profile is provided by the method described in the previous section.

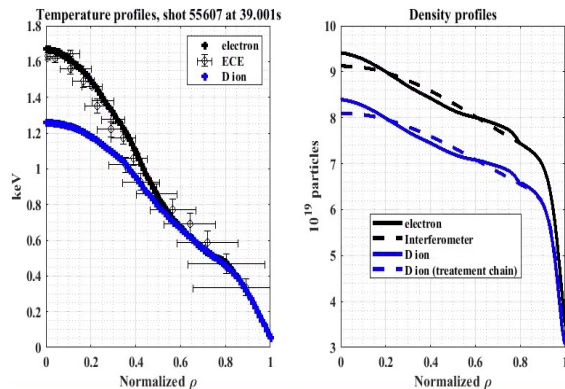


Fig 4: shot #55607 at 39s after 0.5s simulated time. Temperature and density profile compared with ECE and interferometer diagnostics

	Exp.	Sim.
W_{mhd} (MJ)	~0.37	0.31
Neutron rate (10^{11} neutrons/s)	~27	33

Table 2: shot #55607 at 39s after 0.5s simulated time. Comparison of stored energy and neutron rate with experimental data.

Figure 5 (a) and (b) show the presence of the high- k_y electron temperature gradient (ETG). The influence of trapped electron mode (TEM) is small (fig. 5 (a) and (d)). As shown in fig. 5 (a) and (c), the turbulence is dominated by the ion temperature gradient (ITG) instability at low- k_y .

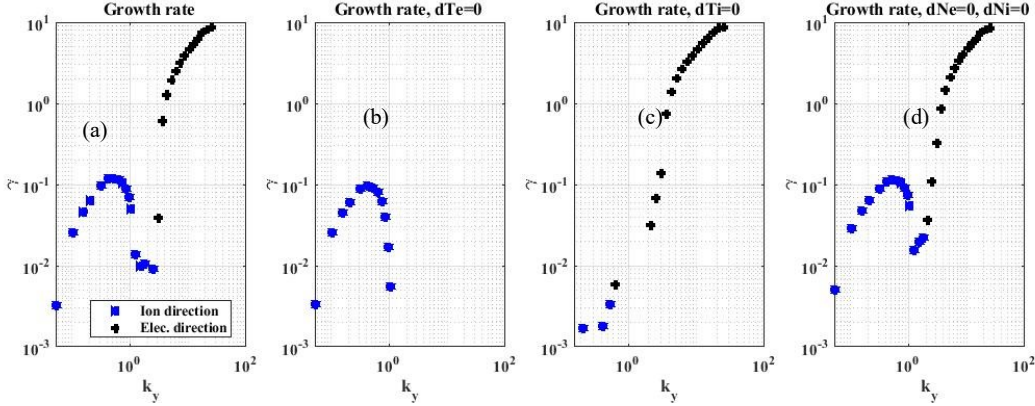


Fig 5: shot #55607 at 39s and normalized $\rho=0.5$. (a) Turbulent linear growth rate γ . (b) Turbulent linear growth rate when T_e gradient is set to 0. (c) Turbulent linear growth rate when T_i gradient is set to 0. (d) Turbulent linear growth rate when N_e and N_i gradients are set to 0. γ is in units of c_s/R with $c_s = \sqrt{T_e/m_e}$, m_i the main ion mass and k_y is the poloidal wave number.

CONCLUSION AND PERSPECTIVES

ETS tools are used to monitor and explain recent WEST experiments. A first validation of ICRF computation with BIS method shows an agreement on the total electron heating at low ICRF power. Further investigations are ongoing. Power and minority scans show that electron heating is always dominant for ICRF power greater than 2-3MW in the studied conditions in particular with H concentration between 5% and 7%. An enhanced D-D neutron rate can be achieved at low H concentrations due to direct N=2 D absorption. Predictive simulation yields a good agreement with available measurements (electron and density temperature profiles, stored energy and neutron rate). The simulation suggests that turbulence is dominated by the ion temperature gradient (ITG) instability at low- k_y . The next step would be to perform self-consistent impurity transport modelling.

REFERENCES

- [1] Kalupin D. et al 2013 *Nucl. Fusion* **53** 123007
- [2] Huynh P. et al 2021 *Nucl. Fusion* **61** 09601
- [3] Bucalossi J. et al 2014 *Fus. Eng. and Design* vol. **89** pp. 907-912
- [4] Bourdelle C. et al 2015 *Nucl. Fusion* **55** 063017
- [5] Lamalle P.U. 1994 *PhD Thesis Universite de Mons LPPER/KMS Report 101*
- [6] Van Eester D. and Lerche E. 2011 *Plasma Phys. Control. Fusion* **53** 09200
- [7] Huynh P. et al 2020 *AIP Conf. Proc.* **2254** 060003
- [8] Van Eester D. et al 2021 *J. Plasma Phys.* vol. **87** 855870202
- [9] Staebler G.M. et al 2007 *Phys. Plasmas* **14** 055909
- [10] Staebler G.M et al 2021 *Plasma Phys. Control. Fusion* **63** 015013
- [11] Dumont R. 2009 *Nucl Fusion* **49** 075033.
- [12] Dumont R. and Zarzoso D. 2012 *Nucl Fusion* **53** 013002.
- [13] Maget P. et al Understanding Tungsten Accumulation during ICRH operation on WEST *this conference 04.129*

ACKNOWLEDGMENTS

This work has been carried out within the framework of the EUROfusion Consortium, funded by the European Union via the Euratom Research and Training Programme (Grant Agreement No 101052200 — EUROfusion). Views and opinions expressed are however those of the author(s) only and do not necessarily reflect those of the European Union or the European Commission. Neither the European Union nor the European Commission can be held responsible for them.